Chemical Physics 463 (2015) 70–81

Contents lists available at ScienceDirect

Chemical Physics

journal homepage: www.elsevier.com/locate/chemphys

Non-equilibrium kinetics, diffusion and heat transfer in shock heated flows of N_2/N and O_2/O mixtures

O. Kunova *, E. Kustova, M. Mekhonoshina, E. Nagnibeda

Department of Mathematics and Mechanics, Saint Petersburg State University, 28, Universitetski pr., Saint Petersburg 198504, Russia

ARTICLE INFO

Article history:
Received 29 July 2015
In final form 11 October 2015
Available online 23 October 2015

Keywords:
State-resolved transport coefficients
State-to-state vibrational kinetics
Heat transfer
Diffusion
Shock waves

ABSTRACT

In this paper, the influence of vibrational and dissociation kinetics on heat transfer and diffusion in non-equilibrium flows of N_2/N and O_2/O mixtures in the relaxation zone behind shock waves is studied on the basis of the state-to-state and one-temperature kinetic theory approaches. The results of calculations of vibrational level populations n_i, gas temperature T, total energy flux $\mathbf{q}$, diffusion velocities of molecules at different vibrational states $\mathbf{V}_i$ and atoms $\mathbf{V}_a$ in the relaxation zone behind a shock front are presented for the free stream Mach numbers $M = 18, 15, 10$. The contribution of different dissipative processes to the total energy flux is evaluated for various flow conditions. Characteristic features of non-equilibrium kinetics, diffusion and energy transfer in two considered mixtures are discussed. The impact of vibrational excitation of N_2 and O_2 molecules in the free stream on a relaxation zone structure and transport properties behind a shock is shown.

1. Introduction

Prediction of gas flow parameters and mass and heat transfer near the Earth re-entering bodies is an important problem of modern physical gas dynamics which has been much discussed in the literature (see bibliography in Refs. [1,2]). State-to-state vibrational kinetics in binary mixtures of shock heated reacting air species [3–6] and in five-component air flows [7,8] has been studied for different free stream conditions using various models for chemical reactions and energy transitions. In recent years the state-to-state description has been extended to ro-vibrational relaxation in air components [9–11]. However, the influence of non-equilibrium molecular distributions in shock heated reacting mixtures on diffusion and heat transfer under re-entry conditions is not sufficiently investigated up to the present time.

During three last decades the classical transport kinetic theory originally developed for weakly non-equilibrium gases has been generalized for reacting mixtures under strongly non-equilibrium conditions in a flow when some kinetic processes proceed in the gas dynamic time scale. Thus, the mathematical transport algorithms for gases with tempered chemical reactions are presented in Ref. [12], the multi-temperature kinetic theory approach is proposed in Ref. [13] and used for shock heated air flows in Ref. [14], the state-to-state transport kinetic theory approach is developed in Ref. [15] and then applied for different flows (see for example Refs. [16–19]).

The objective of the present paper is to explain particular features of diffusion and heat transfer in high-temperature reacting mixtures by analyzing strongly non-equilibrium vibrational distributions in shock heated flows under various initial conditions. As it is already pointed out, the state-to-state vibrational-chemical kinetics in such flows was widely studied in the literature [3–6,9–11,7,8] but this is not the case for transport phenomena. A preliminary study of the heat flux in nitrogen for one specific test case was carried out in Ref. [1] for the reduced model including only 20 vibrational states of N_2 molecules. It is interesting to note that implementation of such a reduced model resulted in overestimated dissociation rates and, as a consequence, overpredicted values of mass diffusion fluxes. In the present study we take into account all vibrational levels up to the dissociation threshold, and analyze diffusive fluxes as well as contributions of heat conduction, mass diffusion and diffusion of vibrational states to the total energy flux in N_2/N and O_2/O mixtures in a wide range of test cases. We show that different rates of energy exchange and chemical reactions in nitrogen and oxygen may lead to significant distinctions in the diffusion and energy transfer; depending on the initial conditions, various dissipative processes become dominating in the heat transfer resulting in strong competition of diffusion and heat conduction.

* Corresponding author.
E-mail addresses: kunova.olga@gmail.com (O. Kunova), elena_kustova@mail.ru (E. Kustova), mekhonoshinama@gmail.com (M. Mekhonoshina), e_nagnibeda@mail.ru (E. Nagnibeda).

http://dx.doi.org/10.1016/j.chemphys.2015.10.004
0301-0104/

Similar approach was applied recently in Refs. [17,18] to study heat transfer in real gas flows on the basis of the state-to-state model. In Ref. [17], a 1D stagnation-line CO_2 flow in a boundary layer was considered, and a strong effect of thermal diffusion on the heat flux is found, comparable to that of heat conduction. In Ref. [18], a 2D low-temperature flow around a blunt body was simulated; it is emphasized that the dominating effect in the heat transfer belongs to heat conduction whereas contributions of mass diffusion and diffusion of vibrational states is negligible. Simulations performed in the frame of the present study reveal quite different physical effects providing insight to the features of heat transfer in high-temperature flows.

Another interesting problem is to understand the impact of initial vibrational excitation of molecules in the free stream on the diffusion and heat transfer. Such a situation may occur in the test section of a supersonic facility, where vibrational degrees of freedom become frozen after expansion [20]. Then initial vibrational non-equilibrium may influence the measured and calculated heat flux on the surface. Several works [21,22] are devoted to this problem. In particular, in Ref. [21] it is shown that neglecting vibrational non-equilibrium before the shock wave yields overpredicted heat transfer rates compared to experimental data. Taking into account vibrational excitation by means of approximate Landau–Teller model [21] provides better agreement with measured heat transfer rates but still leads to some overestimation of the heat flux. It should be noted that diffusion processes were not considered in Refs. [21,22]. In the present paper, we analyze the influence of initial vibrational excitation on the relaxation zone structure and transport properties behind a shock using the state-to-state approach and show that correct simulation of diffusion processes (especially the diffusion of vibrational states) is of great importance for the heat flux prediction. To the best of our knowledge this effect has not been studied earlier.

The paper is organized as follows. In Sections 2–4 we briefly recall the governing equations and give representation for the diffusion velocity and heat flux in the one-temperature and state-to-state models. In Sections 5.1 and 5.2 we present the results obtained for the equilibrium free stream conditions. Analysis of vibrational distributions and macroscopic flow variables performed in 5.1 is then used in 5.2 for the interpretation of particular features of diffusion and heat transfer behind the shock wave. Section 5.3 is devoted to the simulations of test cases with initial vibrational excitation; its effect on the heat transfer is discussed in details.

2. Kinetic scheme and flow equations

Experimental results obtained for high-temperature air species [23,24] show a substantial difference between relaxation times for translational-rotational degrees of freedom (τ_{tr}, τ_{rot}) and vibrational and chemical kinetic processes ($\tau_{vibr}, \tau_{react}$). Therefore in modeling of shock heated flows it is usually supposed that within a thin shock front with the length of about several mean free paths the equilibrium or weakly non-equilibrium distributions over velocities and rotational energies establish whereas vibrational distributions and mixture composition inside the shock front are considered frozen. Then, in the relaxation zone with the length of many hundreds or even thousands of mean free paths, vibrational relaxation and chemical reactions proceed in the strongly non-equilibrium regime with the characteristic time comparable to the mean time of gas flow parameters variation Θ. We consider the flows of N_2/N and O_2/O mixtures in the relaxation zone behind a shock under the condition:

$$\tau_{tr} \lesssim \tau_{rot} \ll \tau_{vibr} < \tau_{react} \sim \Theta \tag{1}$$

providing the basis for the state-to-state flow description.

The kinetic processes included in the mechanism are:

- *VV* vibrational energy exchanges

$$\begin{aligned} &N_2(i) + N_2(k) \leftrightarrow N_2(i \pm 1) + N_2(k \mp 1), \\ &O_2(i) + O_2(k) \leftrightarrow O_2(i \pm 1) + O_2(k \mp 1), \end{aligned} \tag{2}$$

- *VT* vibrational energy transitions for molecules at the *i*th level as a result of collision with an atom (*VTa*) or a molecule (*VTm*)

$$\begin{aligned} &N_2(i) + M \leftrightarrow N_2(i \pm 1) + M, \quad M = N_2, N, \\ &O_2(i) + M \leftrightarrow O_2(i \pm 1) + M, \quad M = O_2, O, \end{aligned} \tag{3}$$

- dissociation and recombination

$$\begin{aligned} &N_2(i) + M = N + N + M, \quad M = N_2, N, \\ &O_2(i) + M = O + O + M, \quad M = O_2, O. \end{aligned} \tag{4}$$

It is worth mentioning that multi-quantum transitions may play essential role in the vibrational kinetics under high temperature conditions, and including them into the kinetic scheme is important for accurate flow simulations. Nevertheless in the present study the main emphasis is given to qualitative estimates of the effect of state-to-state kinetics on the transport properties, and a simplified relaxation mechanism based on single-quantum transitions is used to avoid complications in the calculation of state-to-state transport coefficients. Moreover, at high temperatures ionization and metastable states can have an important role as shown in [25,26]. However the corresponding state-to-state transport theory has not been developed yet up to now. That is why we do not take into account ionization and metastable states in the present study.

Under the condition (1) the sets of flow parameters for considered mixtures include populations $n_i(\mathbf{r}, t)$ of vibrational levels of N_2 or O_2 molecules, number densities $n_a(\mathbf{r}, t)$ of N or O atoms, the gas temperature $T(\mathbf{r}, t)$ and velocity $\mathbf{v}(\mathbf{r}, t)$, $\mathbf{r}$ is the coordinate, t is the time. The system of flow equations is derived from the kinetic equations for distribution functions using the Chapman–Enskog method generalized for conditions of rapid translational-rotational energy exchanges and slow vibrational and chemical processes in the following form [15,1]:

$$\frac{dn_i}{dt} + n_i \nabla \cdot \mathbf{v} + \nabla \cdot (n_i \mathbf{V}_i) = R_i^{VTm} + R_i^{VTa} + R_i^{VV} + R_i^{diss-rec}, \quad i = 0, 1, \ldots l, \tag{5a}$$

$$\frac{dn_a}{dt} + n_a \nabla \cdot \mathbf{v} + \nabla \cdot (n_a \mathbf{V}_a) = -2 \sum_i R_i^{diss-rec}, \tag{5b}$$

$$\rho \frac{d\mathbf{v}}{dt} + \nabla \cdot \mathbf{P} = 0, \tag{5c}$$

$$\rho \frac{dU}{dt} + \nabla \cdot \mathbf{q} + \mathbf{P} : \nabla \mathbf{v} = 0. \tag{5d}$$

Here l is the number of excited vibrational levels for N_2 or O_2 molecules, U is the total energy per unit mass: $\rho U = \frac{3}{2} n k_B T + \rho E_{rot} + \sum_i \varepsilon_i n_i + \varepsilon_a n_a$, ρ and n are the mass and number densities of a gas mixture, k_B is the Boltzmann constant, E_{rot} is the rotational energy per unit mass, ε_i is the vibrational energy of a molecule at the ith vibrational level, ε_a is the formation energy of atoms, $\mathbf{V}_i$ is the diffusion velocity of molecules at the ith vibrational level, $\mathbf{V}_a$ is the diffusion velocity of atoms, $\mathbf{q}$ is the total energy flux, $\mathbf{P}$ is the pressure tensor. In the state-to-state approach the gas temperature T is the translational-rotational temperature. The source

terms in the Eqs. (5a) and (5b) describe the non-equilibrium kinetic processes (2)–(4):

$$R_i^{VTm} = n_{\mathrm{m}} \sum_{i'=i\pm1} \left(n_{i'} k_{i'i}^{\mathrm{m}} - n_i k_{ii'}^{\mathrm{m}}\right), \tag{6a}$$

$$R_i^{VTa} = n_{\mathrm{a}} \sum_{i'=i\pm1} \left(n_{i'} k_{i'i}^{\mathrm{a}} - n_i k_{ii'}^{\mathrm{a}}\right), \tag{6b}$$

$$R_i^{VV} = \sum_k \sum_{i'=i\pm1} \sum_{k'=k\mp1} \left(n_{i'} n_{k'} k_{i'i}^{k'k} - n_i n_k k_{ii'}^{kk'}\right), \tag{6c}$$

$$R_i^{diss-rec} = n_a^2 (n_m k_{rec,i}^{\mathrm{m}} + n_{\mathrm{a}} k_{rec,i}^{\mathrm{a}}) - n_i (n_m k_{i,diss}^{\mathrm{m}} + n_a k_{i,diss}^{\mathrm{a}}). \tag{6d}$$

Here n_m is the number densities of molecules N_2 or O_2, $k_{ii'}^{\mathrm{m}}, k_{ii'}^{\mathrm{a}}, k_{ii'}^{kk'}, k_{i,diss}^{\mathrm{m}}, k_{i,diss}^{\mathrm{a}}, k_{rec,i}^{\mathrm{m}}, k_{rec,i}^{\mathrm{a}}$ are the rate coefficients for vibrational energy transitions (2) and (3), dissociation and recombination (4).

Along with the state-to-state approach we use the one-temperature flow description in terms of number densities of molecules n_m and atoms n_a, gas temperature and velocity [1]. Eq. (5a) are reduced in this case to one equation for n_m:

$$\frac{dn_m}{dt} + n_m \nabla \cdot \mathbf{v} + \nabla \cdot (n_m \mathbf{V}_m) = R_m^{diss-rec} \tag{7}$$

coupled to the equation

$$\frac{dn_a}{dt} + n_a \nabla \cdot \mathbf{v} + \nabla \cdot (n_a \mathbf{V}_a) = -2R_m^{diss-rec} \tag{8}$$

and Eqs. (5c) and (5d).

Source terms in Eqs. (7) and (8) contain one-temperature dissociation and recombination rate coefficients.

3. Diffusion and heat transfer

The expressions for diffusion velocities, total energy flux and pressure tensor in the state-to-state approach are derived in Refs. [15,27,1]. The equations for the diffusion velocities and total energy flux may be written as a sum of contributions of different processes [28]:

$$\mathbf{V}_i = \mathbf{V}_i^{TD} + \mathbf{V}_i^{MD} + \mathbf{V}_i^{DVE}, \tag{9a}$$

$$\mathbf{V}_a = \mathbf{V}_a^{TD} + \mathbf{V}_a^{MD}, \tag{9b}$$

$$\mathbf{q} = \mathbf{q}^{HC} + \mathbf{q}^{MD} + \mathbf{q}^{TD} + \mathbf{q}^{DVE}. \tag{10}$$

Here, $\mathbf{V}_i^{MD}, \mathbf{V}_a^{MD}, \mathbf{V}_i^{TD}, \mathbf{V}_a^{TD}$ and $\mathbf{V}_i^{DVE}$ are, respectively, the contributions of the mass diffusion, thermal diffusion, and diffusion of vibrational energy:

$$\mathbf{V}_i^{MD} = -D_{mm}\mathbf{d}_m - D_{ma}\mathbf{d}_a, \tag{11a}$$

$$\mathbf{V}_i^{TD} = -D_{Tm} \nabla \ln T, \tag{11b}$$

$$\mathbf{V}_i^{DVE} = -n \left(\frac{n_m}{D_{mm}} + \frac{n_a}{D_{ma}}\right)^{-1} \nabla \ln \frac{n_i}{n_m}, \tag{11c}$$

$$\mathbf{V}_a^{MD} = -D_{ma}\mathbf{d}_m - D_{aa}\mathbf{d}_a, \tag{11d}$$

$$\mathbf{V}_a^{TD} = -D_{Ta} \nabla \ln T. \tag{11e}$$

In Eq. (10) $\mathbf{q}^{HC}, \mathbf{q}^{MD}, \mathbf{q}^{TD}$ and $\mathbf{q}^{DVE}$ are, respectively, energy fluxes associated with the heat conductivity of translational and rotational degrees of freedom (Fourier flux), mass diffusion, thermal diffusion, and the transfer of vibrational energy:

$$\mathbf{q}^{HC} = -\lambda' \nabla T, \tag{12a}$$

$$\mathbf{q}^{MD} = \rho_m h_m \mathbf{V}_m^{MD} + \rho_a h_a \mathbf{V}_a^{MD}, \tag{12b}$$

$$\mathbf{q}^{TD} = -p(D_{Tm}\mathbf{d}_m + D_{Ta}\mathbf{d}_a) + \rho_m h_m \mathbf{V}_m^{TD} + + \rho_a h_a \mathbf{V}_a^{TD}, \tag{12c}$$

$$\mathbf{q}^{DVE} = \sum_i \left(\frac{5}{2} k_B T + \langle \varepsilon^i \rangle_{rot} + \varepsilon_i\right) n_i \mathbf{V}_i^{DVE}. \tag{12d}$$

In Eqs. (11) $D_{mm}, D_{ma}, D_{aa}, D_{Tm}$ and D_{Ta} are the multi-component diffusion and thermal diffusion coefficients for each molecule and atom, $\mathbf{d}_m$ and $\mathbf{d}_a$ are the diffusive driving forces depending on gradients of the level populations n_i and atom densities n_a, the pressure $p = nk_BT$. In expression (12a) $\lambda' = \lambda_{tr} + \lambda_{rot}$ is the thermal conductivity coefficient, λ_{tr} and λ_{rot} correspond to energy transfer due to elastic collisions and those with rotational energy transitions. h_m, h_a, ρ_m and ρ_a are the enthalpy per unit mass and the densities of molecular and atomic components, $\langle \varepsilon^i \rangle_{rot}$ is the mean rotational energy.

The peculiar feature of the state-to-state approach is that the total energy flux involves contributions not only of heat conductivity, mass diffusion and thermal diffusion processes but also that of vibrational energy diffusion for molecules at each vibrational level. Expressions (9)–(11), allow one to assess an impact of various vibrational states on the mass diffusion fluxes. Numerical estimates of this new effect are given in Section 5; these estimates are important for the interpretation of the total heat flux carried out further for a wide range of initial conditions. The diffusion velocities include along with the gradients of temperature T and atomic number densities n_a, also the gradients of all vibrational level populations n_i. Diffusion and heat conductivity coefficients depend on level populations, number densities of atoms, the gas temperature and can be found as a solution of transport linear systems derived for the state-to-state approximation in Refs. [15,27]. Coefficients in these systems are specified by the cross sections of more frequent collisions with transitions of translational and rotational energies.

Following accurate transport algorithms for the considered mixture one should solve $l+1$ equations for evaluation of each independent diffusion coefficient and $3l+2$ equations for heat conductivity coefficients where l is the number of excited vibration levels of N_2 or O_2 molecules. After simplifications proposed in Ref. [27], the number of equations for the binary mixture is reduced to 3 and 5 equations, respectively.

The self-consistent approach is based on the direct implementation of the state-to-state kinetic theory algorithms for transport coefficients to the CFD code and requires the solution of transport systems at each space and time step of calculations (see for example Ref. [29]). Moreover, for viscous gases, state-dependent rate coefficients for energy transitions and chemical reactions in Eqs. (6a)–(6d) should be calculated with regard to deviations from Maxwell velocity distributions of colliding molecules [30–32]. This approach is very complicated and extremely time consuming. Therefore in this paper we used the simplified way proposed in Refs. [15,27]. First, vibrational level populations, number densities of atoms, gas temperature and velocity in the relaxation zone behind a shock wave have been computed by solving the system of Euler equations complemented with additional rate equations to account for chemistry and energy transfer. Then, the obtained data have been substituted to the accurate transport systems for calculations of the total energy flux and diffusion velocities of atoms and molecules at different vibrational states.

In the one-temperature approach the total energy flux and diffusion velocities $\bar{\mathbf{V}}_m$ are presented as a sum of mass diffusion and thermal diffusion:

$$\bar{\mathbf{V}}_m = \bar{\mathbf{V}}_m^{TD} + \bar{\mathbf{V}}_m^{MD}, \tag{13}$$

$$\bar{\mathbf{q}} = \bar{\mathbf{q}}^{HC} + \bar{\mathbf{q}}^{MD} + \bar{\mathbf{q}}^{TD}. \quad (14)$$

It should be noted that contrarily to the state-to-state flow description, in the one-temperature approach transport coefficients are specified by collision cross sections for not only translational and rotational energy transitions but also for the vibrational energy transfer. Representation of mass and energy fluxes in thermally equilibrium air flows in the form (13) and (14) was not implemented before. However it appears rather convenient for the comparison of mass and heat transfer in the frame of accurate state-to-state and simplified one-temperature approaches allowing for assessment of strongly non-equilibrium effects.

4. Vibrational-dissociation kinetics behind a shock front

The equations for the flows of $N_2(i)$/N and $O_2(i)$/O mixtures in the relaxation zone behind a plane shock wave in the Euler approximation follow from the Eqs. (5) [1]:

$$\frac{d(vn_i)}{dx} = R_i^{VTm} + R_i^{VTa} + R_i^{VV} + R_i^{diss-rec}, \quad i = 0, 1, \ldots l, \quad (15a)$$

$$\frac{d(vn_a)}{dx} = -2\sum_i R_i^{diss-rec}, \quad (15b)$$

$$\rho_0 v_0^2 + p_0 = \rho v^2 + p, \quad (15c)$$

$$h_0 + \frac{v_0^2}{2} = h + \frac{v^2}{2}, \quad (15d)$$

where x is the distance from the shock front, the subscript "0" denotes the parameters in the free stream. In Eq. (15d)

$$h = h_m Y_m + h_a Y_a, \quad (16)$$

$Y_m = \rho_m/\rho$ and $Y_a = \rho_a/\rho$ are the mass fractions of molecules and atoms,

$$h_a = \frac{5}{2}\bar{R}_a T + \frac{\varepsilon_a}{m_a}, \quad (17)$$

$$h_m = \frac{7}{2}\bar{R}_m T + \frac{1}{\rho_m}\sum_i \varepsilon_i n_i, \quad (18)$$

where $\bar{R}_m$ and $\bar{R}_a$ are the specific gas constants of molecules N_2, O_2 and atoms N, O, m_a is the atom mass. In calculations the vibrational energies are simulated by the anharmonic and harmonic oscillator models with $l_{N_2} = 46$, $l_{O_2} = 35$ and $l_{N_2} = 32, l_{O_2} = 25$ respectively and the influence of anharmonic effects on flow parameters and transport properties is estimated.

The right hand sides of Eqs. (15a) and (15b) are given by the relations (6a)–(6d). The rate coefficients for vibrational energy transitions are calculated using the generalized formulas of SSH theory [33,23], dissociation rate coefficients are found with the use of the Treanor–Marrone model [34] modified for the state-to-state approach [1]. For recombination rate coefficients the detailed balance principle [1] is used.

The one-temperature approach describes thermally equilibrium flow. In this case just from the beginning of the relaxation zone, vibrational level populations have the form of the Boltzmann distributions which are supposed to establish within the shock front. Consequently Eq. (15a) are reduced to the equation for n_m:

$$\frac{d(vn_m)}{dx} = R_m^{diss-rec}, \quad (19)$$

and the specific vibrational energy in Eq. (18) has the form

$$\frac{1}{\rho_m}\sum_i \varepsilon_i n_i = \frac{1}{m_m}\frac{1}{Z_{vibr}(T)}\sum_i \varepsilon_i \exp\left(-\frac{\varepsilon_i}{k_B T}\right), \quad (20)$$

where $Z_{vibr}(T)$ is the vibrational partition function.

Comparison of the results obtained implementing the state-to-state and one-temperature flow descriptions permitted us to assess the influence of non-equilibrium effects not only on gas-dynamic parameters (which was done earlier in a number of papers) but also on the mass and energy fluxes in nitrogen and oxygen mixtures. It is worth noting that state-to-state diffusion and heat transfer in shock heated oxygen was not studied before. In Section 5 we show a quite different behavior of mass and energy fluxes in oxygen and nitrogen in both state-to-state and one-temperature approaches.

5. Results and discussion

In this section we report the results obtained for two considered mixtures solving numerically Eqs. (15) for the following conditions in a free stream: $M_0 = 18, 15, 10, T_0 = 271$ K, $p_0 = 100$ Pa, $n_a(0) = 0, n_m(0) = p_0/k_B T_0$. We study the relaxation processes and compare the results obtained in the frame of the state-to-state and one-temperature kinetic theory approaches, using the anharmonic and harmonic oscillator models for molecular vibrations, for different Mach numbers before the shock front and equilibrium and non-equilibrium vibrational molecular distributions in the free stream. The influence of these effects on kinetic and transport processes behind the shock wave is analyzed below.

In the state-to-state approach the flow parameters just behind the shock front are found using the Rankine–Hugoniot relations with frozen vibrational distributions and mixture composition within the front.

In the one-temperature approach, chemical composition does not change within the shock front whereas level populations just behind the shock follow the Boltzmann distributions

$$n_{N_2 i} = \frac{n_{N_2}}{Z_{vibr}^{N_2}(T)} \exp\left(-\frac{\varepsilon_i^{N_2}}{k_B T}\right), \quad (21a)$$

$$n_{O_2 i} = \frac{n_{O_2}}{Z_{vibr}^{O_2}(T)} \exp\left(-\frac{\varepsilon_i^{O_2}}{k_B T}\right), \quad (21b)$$

with the gas temperature $T = T_1$ (subscript "1" corresponds to the parameters at $x = 0$) specified by the Mach number and found from the conservation equations taking into account (16), (18) and (20).

Systems (15) and (19), (15b)–(15d) have been solved numerically using the MATLAB `ode15s` multistep solver based on the numerical differentiation formulas. It is efficient for stiff systems of ordinary differential equations and allows us to economize computing time and achieve high computational accuracy (the error does not exceed 10^{-10}% for conservation laws).

5.1. The effect of free stream conditions

First, we consider the traditional case of equilibrium free stream conditions when vibrational level populations before the shock have the form of the Boltzmann distributions (21) with the temperature $T = T_0$.

To validate the method of simulation we compared the results obtained recently in Refs. [10,11,35] to our solution of system (15) under the same initial conditions. In Refs. [10,11], the detailed numerical study of ro-vibrational relaxation in N_2/N mixtures is based on master equations for distributions over rotational and vibrational energies with the use of accurate state-dependent transition rate coefficients[9]. The assessment of translational, vibrational temperatures and N mole fraction showed similar qualitative behavior of flow parameters behind the shock wave and close values of the relaxation zone length. Some quantitative

discrepancy in the fluid dynamic variables near the shock front caused by using different sets of rate coefficients does not modify considerably the characteristic features of mass and heat transfer, which is the main focus of the present study. In Ref. [35], the vibrational temperature T_v and dissociation rate were determined behind the shock wave front in undiluted oxygen by means of experimental study of oxygen absorbance. The comparisons of T_v for different conditions demonstrate satisfactory agreement between the experimental data and our simulations.

The gas temperature variation in N_2/N and O_2/O mixtures found for $M_0 = 18, M_0 = 15$, and $M_0 = 10$ in the state-to-state approach with respect to the distance from the shock front is plotted in Fig. 1. For all three Mach numbers we can see more rapid decrease in the gas temperature for O_2/O mixture than for N_2/N mixture in the beginning of the relaxation zone and then the gas temperature in N_2/N mixture remains about twice higher than that for O_2/O mixture for $M_0 = 18$ and $M_0 = 15$. It is explained by more rapid vibrational excitation of O_2 molecules and therefore their efficient dissociation. As it is expected, dissociation and vibrational relaxation proceed more intensively for the highest Mach number $M_0 = 18$. In the case $M_0 = 10$ the gas temperature practically does not change in N_2/N mixture and changes very slightly in O_2/O mixture.

In Fig. 2 number densities of nitrogen and oxygen atoms are presented in dependence of x for different Mach numbers. The curves show, again, very slow dissociation of N_2 molecules for $M_0 = 10$ and considerably more active dissociation of O_2 molecules for all three cases. It may be noticed that the difference between n_O values found for $M_0 = 18$ and $M_0 = 15$ for $x > 0.1$ cm remains within an order of magnitude whereas for n_N the discrepancy is greater and exceeds two orders of magnitude.

Level populations of nitrogen and oxygen molecules in the relaxation zone are given in Fig. 3(a and b) for $i = 0$ and $i = 10$ and different M_0. Non-monotonic variation of populations for non-zero levels is found more noticeable for O_2 molecules; this behavior reflects the rapid increase in populations due to vibrational excitation and then the decrease as a result of dissociation and deactivation of excited molecules. The zone of vibrational and chemical relaxation in O_2/O mixture occurs noticeably more narrow than that in N_2/N mixture.

Now let us discuss the transport properties calculated using the post-processing procedure described in Section 3. Note that a preliminary study of the heat flux in nitrogen for one specific test case $M = 15$ was carried out in Ref. [1]. In that study, a reduced model

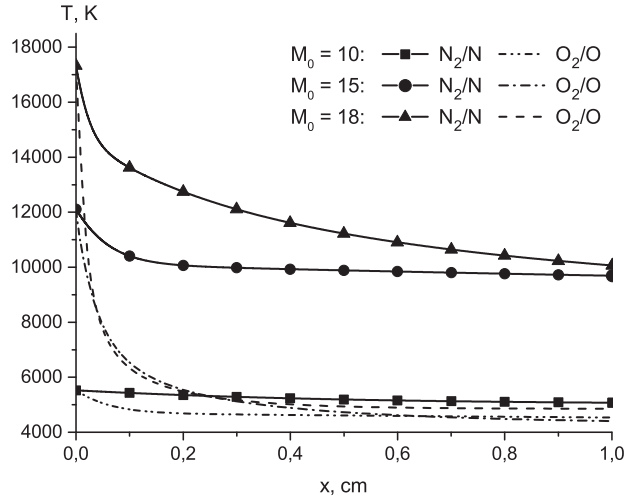

Fig. 1. The temperature T behind the shock front as a function of x.

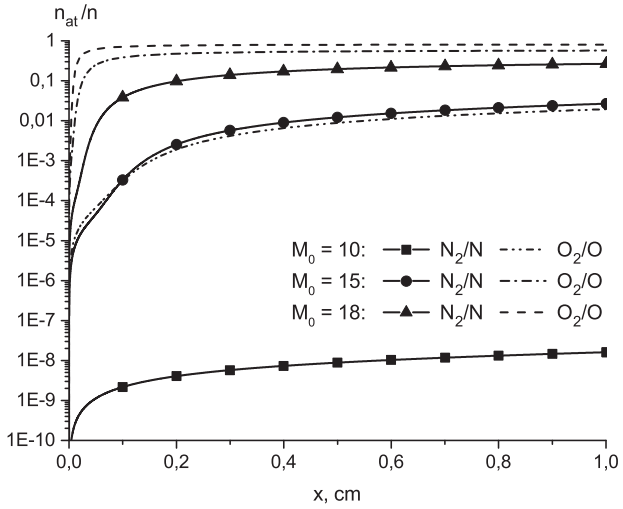

Fig. 2. The atomic molar fractions n_N/n and n_O/n behind the shock front as functions of x.

including only first 20 vibrational states of N_2 molecules was implemented. In the present paper we take into account all vibrational levels, and this changes considerably the total heat flux as is seen below.

In Fig. 4 we plot the mass diffusion flux for atoms $n_a\mathbf{V}_a/n$ and diffusion fluxes for different molecular vibrational states $n_i bf V_i/n$ obtained for $M_0 = 18$. It is seen that the mass diffusion flux for nitrogen atoms is almost zero since dissociation of N_2 molecules is rather slow; for both mixtures $n_a\mathbf{V}_a/n$ is small near the shock front due to the existence of finite incubation time for the dissociation reaction. The absolute value of the mass diffusion flux for oxygen atoms has a maximum at $x \approx 0.02$ cm and after that decreases since the gradients of molar fractions become small far from the shock front. The effect of high vibrational states on the diffusion processes is found to be weak; the most important contribution is given by $i = 0$ and $i = 1$. It is worth mentioning that diffusion processes are of importance only close to the shock front, their contribution tends rapidly to zero with x. Since vibrational excitation proceeds faster in oxygen, the values of $n_i\mathbf{V}_i/n$ are greater in O_2/O mixture.

Fig. 5 presents the variation of the total heat flux in the relaxation zone for different initial conditions. We can see that for $M_0 = 10$, the heat flux is practically zero for both mixtures since the gradients of all gas-dynamic parameters are small. In N_2/N mixture for $M_0 = 15$ the total heat flux varies strongly near the shock front, then (for $x > 0.2$ cm) it rapidly decreases. It should be noted that the heat flux obtained for a $M = 15$ nitrogen flow in Ref. [1] by implementing reduced vibrational ladder is considerably higher than that given in Fig. 5a. The reason for such a discrepancy is that the reduced model overestimates dissociation rates and, as a consequence, overpredicts values of mass diffusion fluxes which become dominating close to the shock front. The most interesting case corresponds to N_2/N mixture at $M_0 = 18$ and O_2/O mixture at $M_0 = 15$ and 18. One can notice non-monotonic behavior of the total heat flux with x explained by the strong competition of different dissipative processes near the shock front. Peculiarities of heat conduction and diffusion processes for the case $M_0 = 18$ and $M_0 = 10$ are discussed in details in the next sections.

5.2. The effect of kinetic description and anharmonicity of molecular vibrations

In this Section, we study the influence of kinetic approach and modelling of vibrational spectrum on gas-dynamic

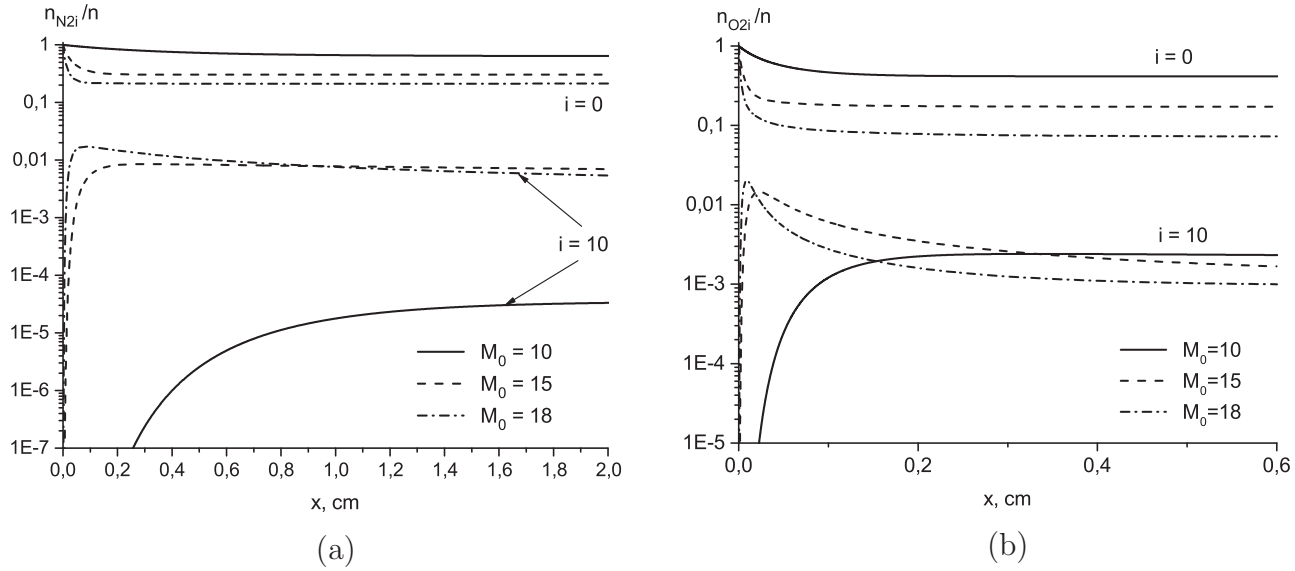

Fig. 3. The vibrational level populations $n_{N_2 i}/n$ (a) and $n_{O_2 i}/n$ (b) as functions of x.

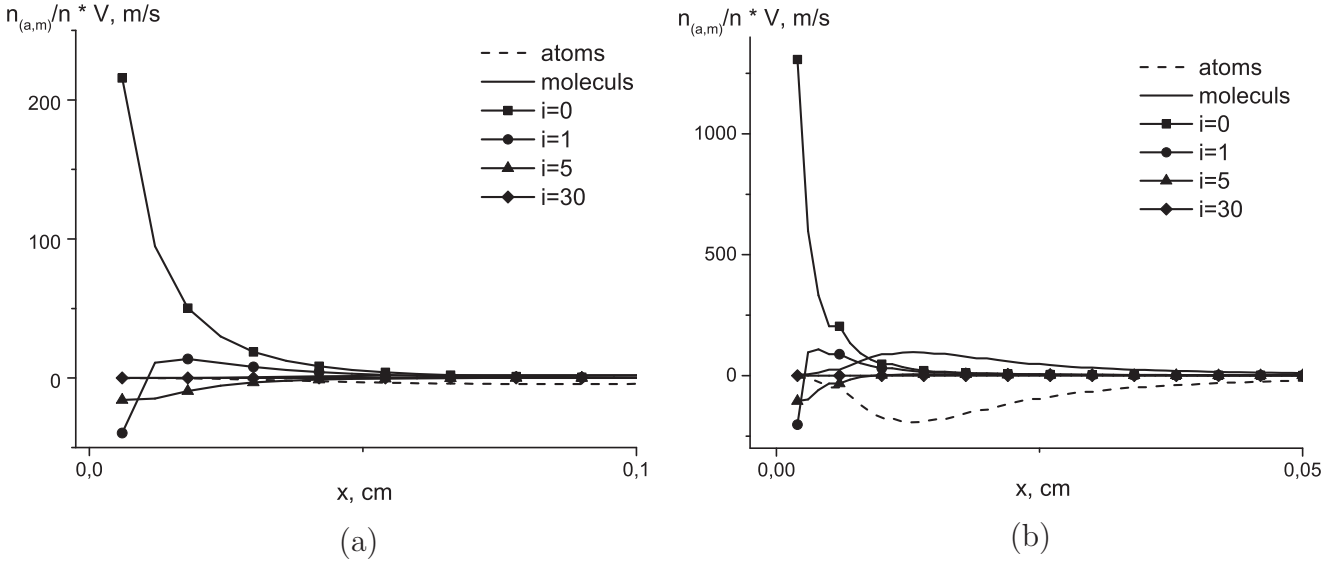

Fig. 4. The diffusion fluxes behind the shock as functions of x for $M_0 = 18$. (a): N_2/N, (b): O_2/O.

parameters and transport properties. Comparison of the gas temperature and number densities of atoms obtained in the frame of the state-to-state and one-temperature approaches with the use of the anharmonic and harmonic oscillator models is shown in Figs. 6(a and b) and 7(a and b) for $M_0 = 18$. Implementation of the one-temperature model leads to a considerable underestimation of the gas temperature behind the shock compared to the case of state-to-state description since in the thermally equilibrium mixture the molecular vibrational states are completely excited already at $x = 0$ as a result of rapid TV translation-vibrational energy transfer within the shock front. Due to the same reason the one-temperature model noticeably overestimates number densities of atoms and does not describe the delay of dissociation in the beginning of the relaxation zone; the existence of a finite incubation time demonstrated experimentally [23] is well described by the state-to-state approach. This effect is discussed previously for shock heated N_2/N [1] and N_2/O_2/NO/N/O mixtures [7].

The anharmonicity of vibrations influences more noticeably the gas temperature and atom number densities in the N_2/N mixture. The discrepancies between the gas temperature and atomic number density values in the N_2/N mixture obtained for anharmonic and harmonic oscillators reach 6% and 16%, respectively. For the one-temperature approach, we do not plot the comparison of flow parameters for the harmonic and anharmonic oscillators since the difference is found to be negligible.

Level populations of N_2 and O_2 molecules as functions of vibrational energies are reported in Fig. 8(a and b) for several positions behind the shock wave. Quite different behavior of level populations is found for the state-to-state and one-temperature approaches. While the state-to-state level populations vary with x non-monotonically, the one-temperature thermally equilibrium distributions are already excited just behind the shock and decrease starting from the beginning of the relaxation zone due to dissociation. Close to the shock front one-temperature distributions exceed considerably state-to-state level populations but with

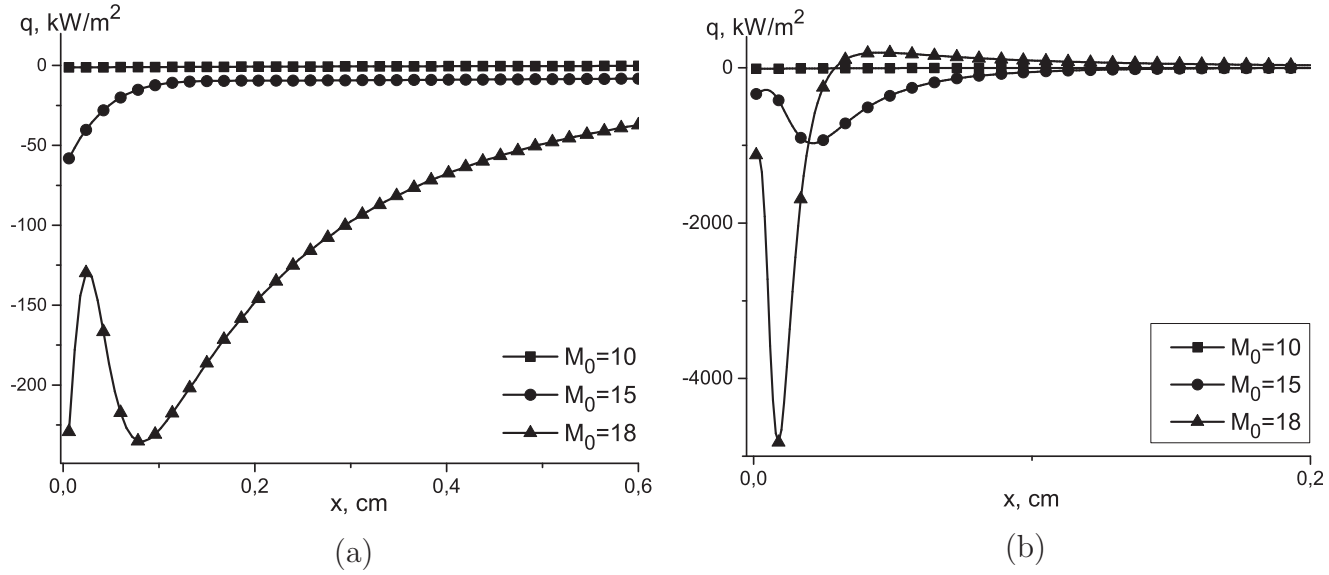

Fig. 5. The total heat flux behind the shock as a function of x. (a): N_2/N, (b): O_2/O.

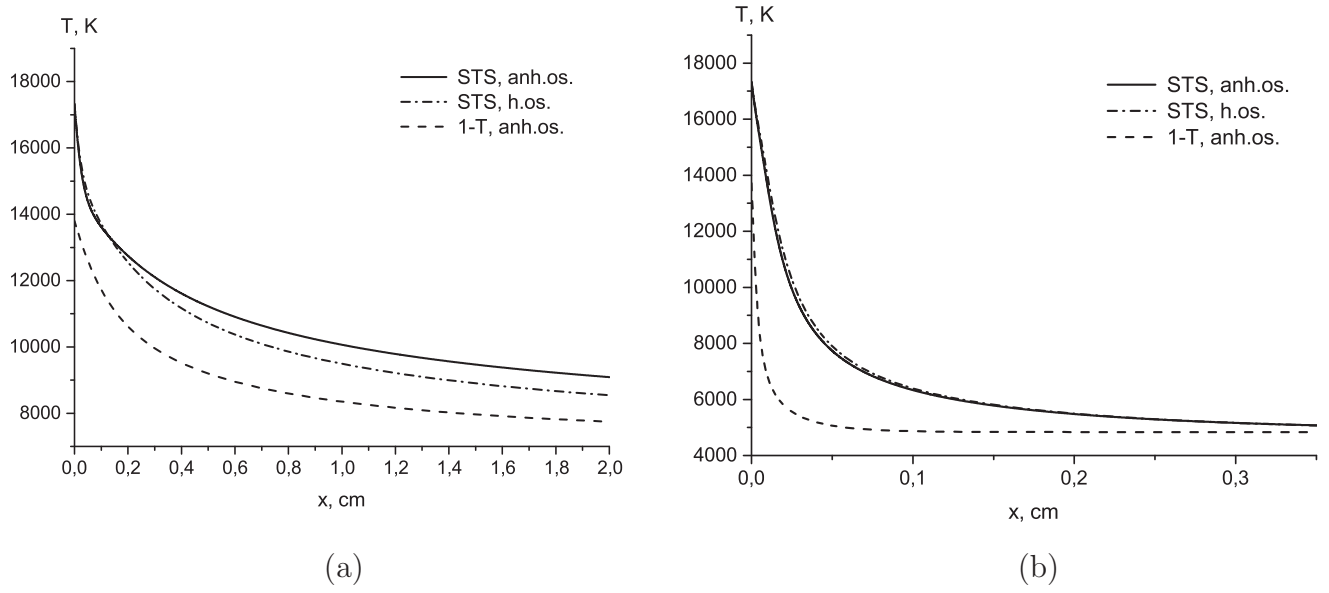

Fig. 6. The temperature T as a function of x for $M_0 = 18$. (a): N_2/N, (b): O_2/O.

x rising they become lower. Neglecting the anharmonicity results in underestimation of the level populations for excited states.

In Fig. 9 we compare the total heat flux calculated using different kinetic approaches and models for vibrational spectra at $M_0 = 18$. In the case of one temperature description, the absolute value of the total heat flux decreases monotonically with x whereas in the state-to-state approach it behaves non-monotonically. Moreover, the absolute value of the heat flux calculated in the one temperature approach is considerably higher for both N_2/N and O_2/O mixtures. The effect of anharmonicity in the state-to-state approach is found to be important close to the shock front where it shifts the peaks in the heat flux values; however it becomes small with the distance: the effect does not exceed 2% for $x > 0.3$ cm in the case of N_2/N mixture and for $x > 0.05$ cm in the case of O_2/O mixture. For the one-temperature description, the results obtained for harmonic and anharmonic oscillators practically coincide.

It is interesting to understand the reason for different behavior of the total heat flux found for various initial conditions and kinetic models. For this purpose, we assess the contributions of multiple dissipative processes to the total energy flux according to Eq. (10). The results for $M_0 = 18$ are presented in Fig. 10.

First, for all cases considered, we found that thermal diffusion has practically no effect on the heat flux behind the shock wave. Therefore we do not plot $\mathbf{q}^{TD}$ in the next figures. Let us discuss now the contributions of other processes. Consider the case of N_2/N mixture in the state-to-state approach. The Fourier flux due to heat conductivity $\mathbf{q}^{HC}$ and the flux caused by the diffusion of vibrational energy $\mathbf{q}^{DVE}$ give the contribution of the same order near the shock front and their absolute values are rather high at $x < 0.1$ cm. Nevertheless the signs of these terms are opposite which causes a strong compensation effect leading to much lower values of the total flux $\mathbf{q}$. The contribution of the vibrational energy diffusion to the heat flux in shock heated flows occurs larger, and it

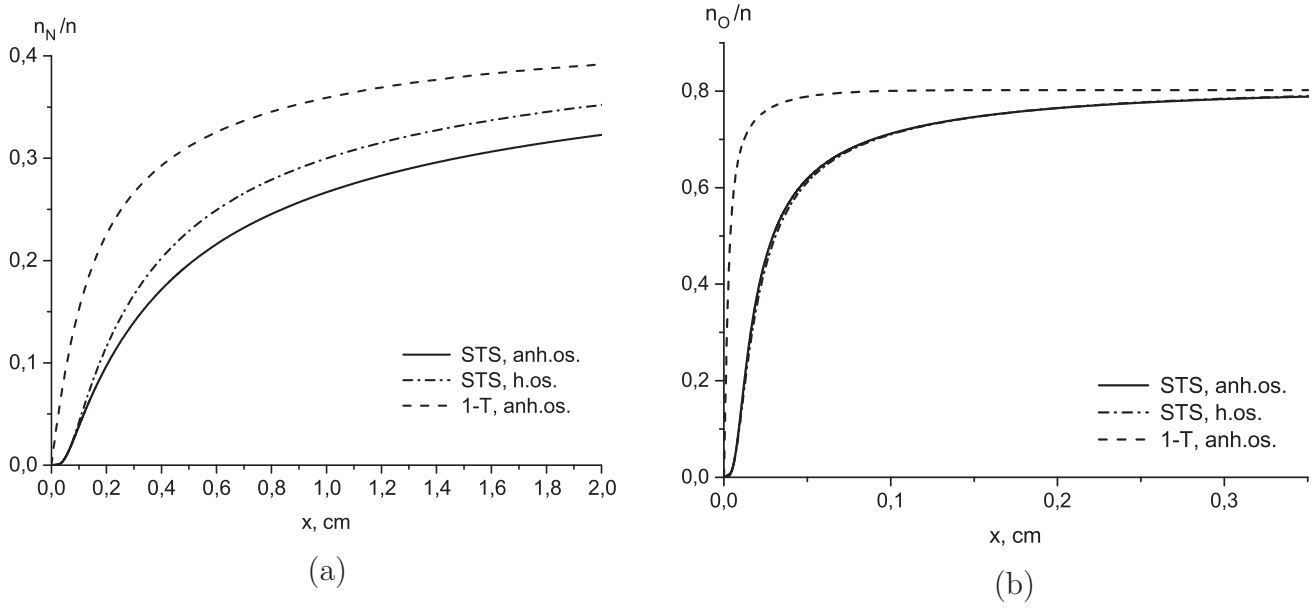

Fig. 7. The atomic molar fractions n_N/n (a) and n_O/n (b) as functions of x for $M_0 = 18$.

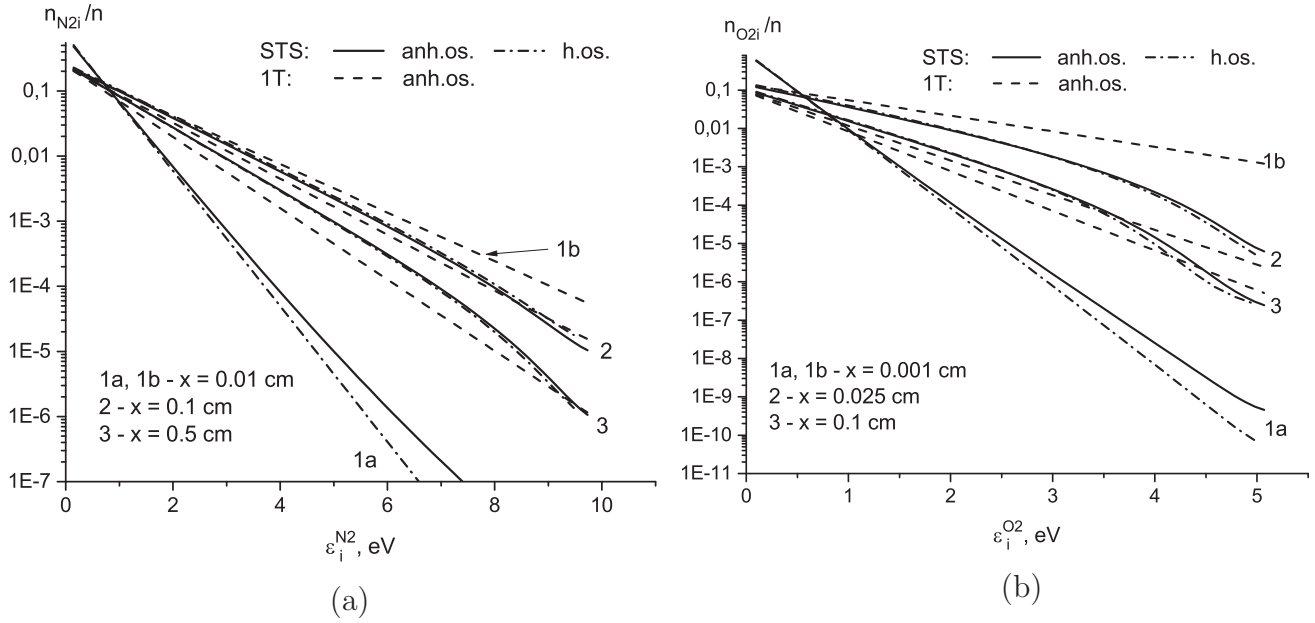

Fig. 8. The vibrational distributions n_{Ni}/n (a) and n_{Oi}/n (b) for different values of x for $M_0 = 18$.

leads to switching the sign of **q** compared to that of the Fourier flux, that is why the total energy flux is negative. The influence of mass diffusion becomes noticeable only at $x > 0.05$ cm due to the dissociation incubation time. It is worth noting that the increase in the heat flux absolute value at $x > 0.05$ cm is connected to the increasing role of mass diffusion. Thus the total heat flux behavior in the state-to-state approach is non-monotonic with x for $M_0 = 18$. For lower Mach numbers, dissociation of N_2 molecules is not enough efficient to provide a considerable effect of mass diffusion; as a consequence, the heat flux decreases monotonically with the distance.

In the one temperature approximation, the Fourier heat flux includes the transfer of vibrational energy specified by the corresponding heat conductivity coefficient; the diffusion of vibrational states is not considered as a separate contribution to the total flux. One can notice that in the one-temperature approach, the role of mass diffusion is much more important: the absolute value of $\mathbf{q}^{MD}$ is about twice larger than $\mathbf{q}^{HC}$ near the shock front. It is not surprising since in thermally equilibrium gas dissociation starts immediately behind the shock front (see also Fig. 7), and the gradients of species molar fractions are rather high. Thus the main process determining the heat transfer in a high-temperature thermal equilibrium flow is mass diffusion.

In Fig. 10(b) we present the same contributions to the heat flux in O_2/O mixture. One can see that qualitatively this case is very similar, but all the processes occur faster and the gradients of gas-dynamic variables are larger compared to those in the case of N_2/N mixture. As a result, the absolute value of the total heat flux is higher and equilibrium is attained earlier. Fast dissociation of oxygen molecules causes stronger effect of mass diffusion on

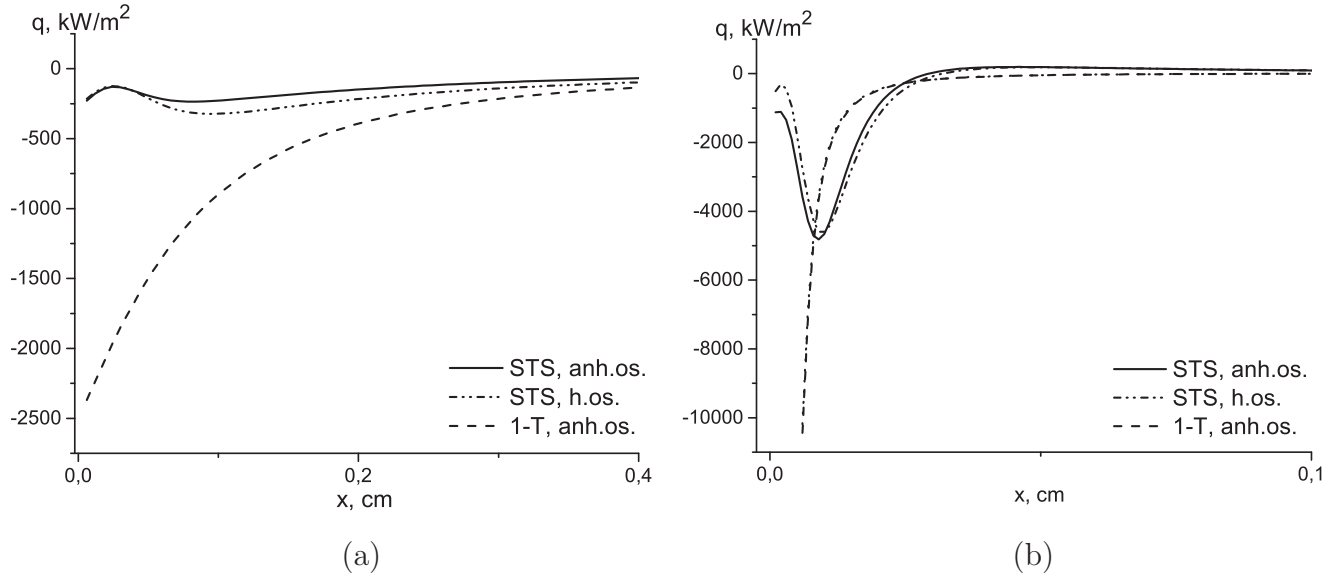

Fig. 9. The total heat flux behind the shock as a function of x. $M_0 = 18$. (a): N_2/N, (b): O_2/O.

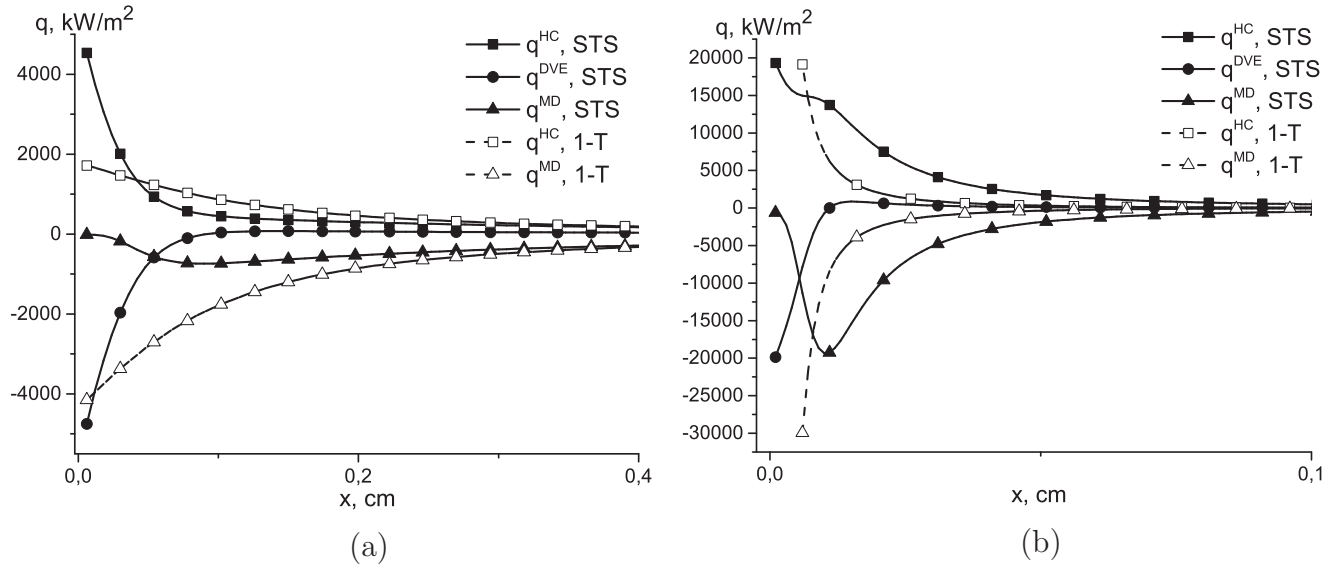

Fig. 10. The contribution of various processes to the heat flux as a function of x. $M_0 = 18$. (a): N_2/N, (b): O_2/O.

the heat transfer. The situation is similar for the case $M_0 = 15$ thus explaining the non-monotonic total heat flux in oxygen (see Fig. 5).

5.3. The effect of vibrationally non-equilibrium free stream conditions

Now we will show the variation of flow parameters, vibrational distributions and heat fluxes behind a shock wave originated in a non-equilibrium free stream. Such conditions may occur as a result of vibrational energy pumping in the free stream (in the ground test facilities, in the flows near bodies of complicated form) and may be important for the chemical reactions control in a shock heated gas. In this case vibrational level populations before the shock front are described by the non-equilibrium Boltzmann distributions with the vibrational temperatures $T_v^{N_2}$ and $T_v^{O_2}$ which are higher than the gas temperature T_0:

$$n_{N_2 i} = \frac{n_{N_2}}{Z^{N_2}_{vibr}(T_v^{N_2})} \exp\left(-\frac{\varepsilon_i^{N_2}}{k_B T_v^{N_2}}\right), \tag{22a}$$

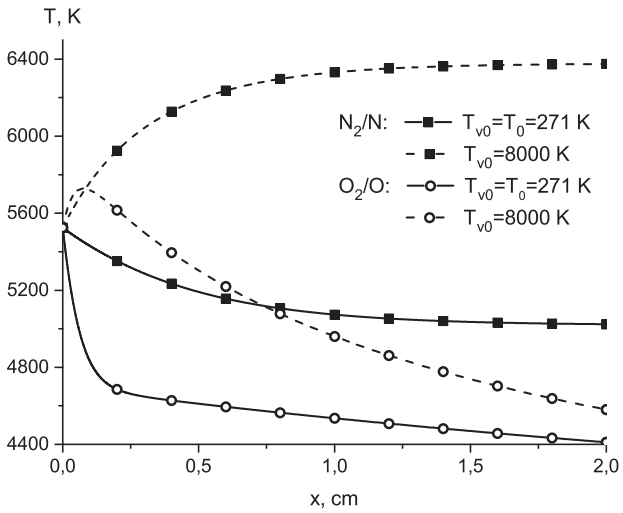

Fig. 11. The temperature T as functions of x for $M_0 = 10$.

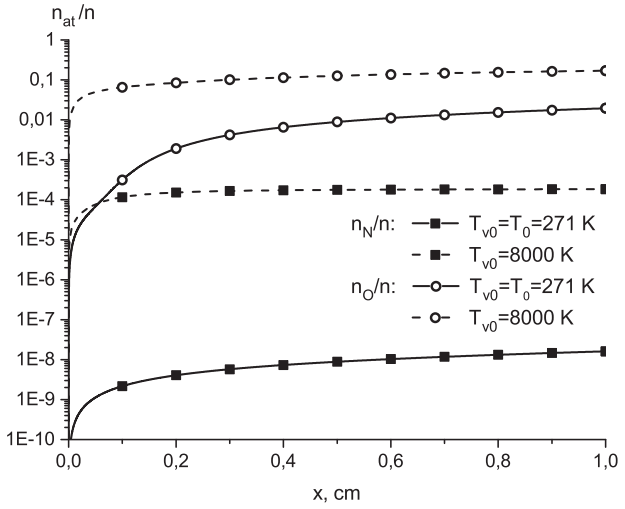

Fig. 12. The atomic molar fractions n_N/n and n_O/n behind the shock front as functions of x for $M_0 = 10$.

$$n_{O_2 i} = \frac{n_{O_2}}{Z^{O_2}_{vibr}(T_v^{O_2})} \exp\left(-\frac{\varepsilon_i^{O_2}}{k_B T_v^{O_2}}\right). \tag{22b}$$

Distributions (22) specify a contribution of vibrational energy to the initial total enthalpy h. We consider two cases for $M_0 = 10$:

(1) equilibrium free stream ($T_v^{N_2} = T_v^{O_2} = T_0$);
(2) vibrationally excited free stream molecules ($T_v^{N_2} = T_v^{O_2} = T_v = 8000$ K).

Other conditions before a shock are the same for both cases and given above. In the second case, the flow parameters in the relaxation zone are determined not only by the value T_1 depending on the Mach number before the shock front but also by the initial vibrational temperature. In Figs. 11 we compare the change in the gas temperature for two considered cases. In the first case the temperature T_1 just behind a shock is higher than T_v ($T_1 > T_v = T_0$) and the gas temperature decreases with x due to the loss of the translational energy in (TV) vibrational excitation and dissociation. In the second case the temperature T_1 occurs considerably less than T_v ($T_1 < T_v$) and the high vibrational energy of initially excited molecules transfers to the translational one in (VT) deactivation process. It is interesting that in the second case the gas temperature variation is found quite different for two mixtures. In N_2/N mixture the temperature noticeably increases behind the shock and then decreases very slightly because N_2 dissociation proceeds weakly. On the contrary, in O_2/O mixture the gas temperature increases due to VT energy transfer from vibrationally excited molecules in a very thin layer behind the shock front and then noticeably decreases because of dissociation.

A substantial difference in atom densities and vibrational distributions of N_2 and O_2 molecules found for the equilibrium and non-equilibrium free stream conditions is shown in Figs. 12 and 13(a and b) respectively. In the second case ($T_1 < T_v$) dissociation of vibrationally excited molecules starts just from the beginning of the relaxation zone and proceeds very intensively close to the shock front particularly for O_2 molecules. In this case there is no delay of dissociation found for the first case ($T_1 > T_v = T_0$). As a result atom densities (Fig. 12) and level populations (Fig. 13(a and b)) in the second case occur much higher than in the first case. With x rising this difference decreases more rapidly in the flow of O_2/O mixture than for N_2/N mixture.

We would like to emphasize that the final equilibrium values of the gas temperature, number densities of species and level populations calculated for the thermally and chemically equilibrium flow occur different for two considered cases of free stream conditions because of the vibrational energy contribution to the total energy before the shock wave in the second case.

Before proceeding to the discussion of heat transfer in a flow under initial vibrational non-equilibrium it is worth to note that a similar problem was analyzed in Ref. [21]. In this reference, the effect of vibrational non-equilibrium on the heat transfer in a hypersonic double-cone flow is assessed. It is shown that neglecting vibrational excitation occurring in the test section after the nozzle expansion results in the overestimated heat transfer rate compared to measured values. Taking into account vibrational excitation by means of approximate Landau–Teller model provides better agreement with measured heat transfer rates but still leads to some overestimation of the heat flux. We would like to

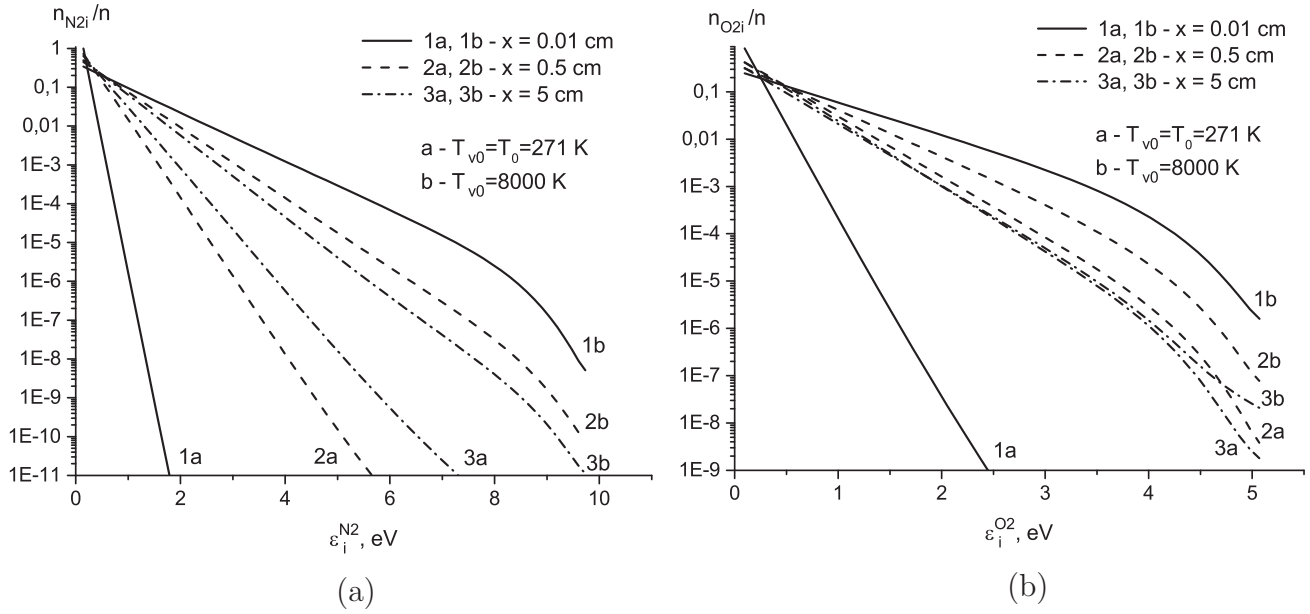

Fig. 13. The vibrational distributions n_{Ni}/n (a) and n_{Oi}/n (b) for different values of x for $M_0 = 10$.

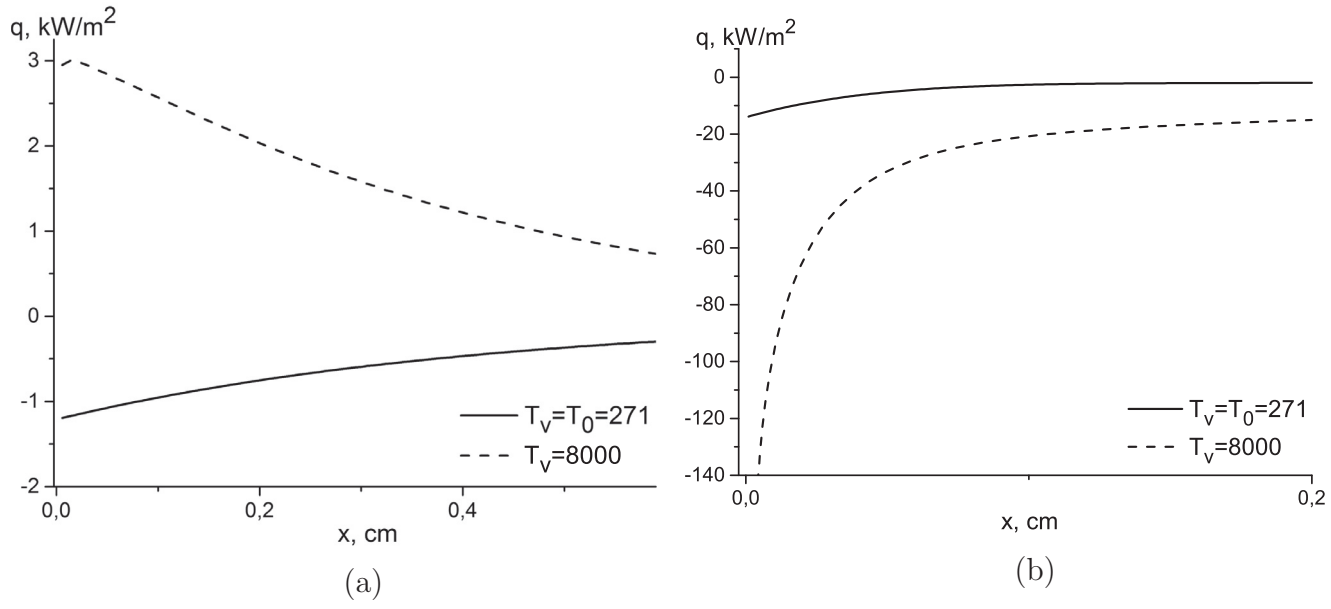

Fig. 14. The total heat flux behind the shock as a function of x. $M = 10$. (a): N_2/N, (b): O_2/O.

emphasize that in Ref. [21], diffusion of vibrational energy is not considered since the multi-temperature flow description is used in simulations. On the other hand as we have seen above, diffusion processes, and especially energy transfer by vibrationally excited states, may significantly modify the heat flux and improve the predicted rates of heat transfer. Moreover, using in Ref. [21] of the Landau–Teller model developed originally for weak deviations from equilibrium may result in a considerable overestimation of the vibrational relaxation rate in the case of highly elevated vibrational temperature [31] thus increasing the calculated heat transfer rate. In the present study we overcome these limitations applying the accurate state-to-state kinetic and transport model for simulating both gas dynamics and mass and energy transport.

The total heat flux for equilibrium ($T_0 = T_v = 271$ K) and strongly non-equilibrium ($T_0 = 271$ K, $T_v = 8000$ K) initial conditions is presented in Fig. 14. Although for $M = 10$ the heat flux is very small the strongly non-equilibrium case is still interesting for the qualitative analysis. For the initially non-equilibrium N_2/N mixture flow the heat flux changes its sign and becomes positive in contrast to the negative heat flux in the first case (Fig. 14(a)). On the other hand, for O_2/O mixture the absolute value of the total heat flux in initially non-equilibrium flow becomes by an order of magnitude greater, however its sign does not change (Fig. 14(b)).

Such peculiarities can be understood analysing different contributions to the heat flux. For N_2/N mixture (Fig. 15(a)) the influence of mass diffusion on the total heat flux is small, the Fourier flux and the flux caused by vibrational energy diffusion make the contributions of the same order near the shock front ($x < 0.2$ cm), but the effect of diffusion is stronger. Therefore the sign of the total heat flux is determined by $\mathbf{q}^{DVE}$. For strongly non-equilibrium case, both the Fourier flux and the flux caused by diffusion of vibrational energy reverse their signs since the excitation processes are

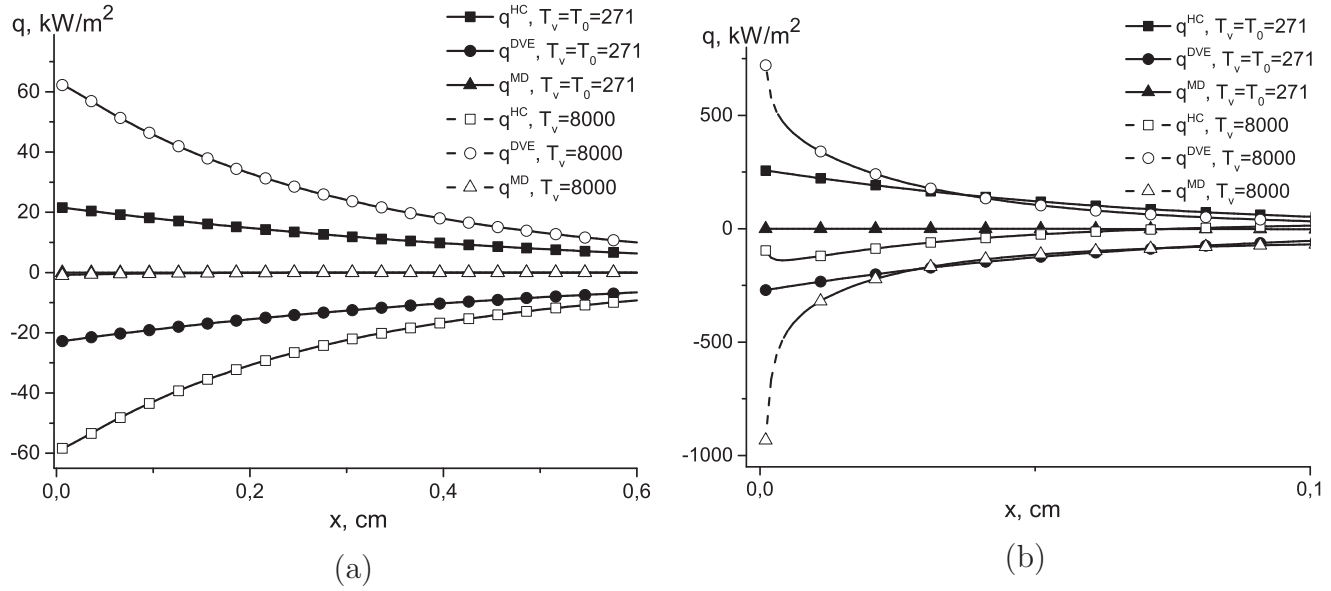

Fig. 15. The contribution of the various processes in the heat flux behind the shock as a function of x. $M = 10$. (a): N_2/N, (b): O_2/O.

replaced by deactivation, and the gas temperature increases with x (Fig. 11). For O_2/O mixture (Fig. 15(b)) initial vibrational non-equilibrium enhances dissociation, and the main contribution to $\mathbf{q}$ belongs to mass diffusion. Although the Fourier flux and the flux of vibrational energy change their signs, the sign of the total heat flux is specified by $\mathbf{q}^{MD}$ which absolute value exceeds considerably those of $\mathbf{q}^{HC}$ and $\mathbf{q}^{DVE}$.

6. Conclusions

The influence of state-to-state vibrational-dissociation kinetics in the flows of binary mixtures $N_2(i)$/N and $O_2(i)$/O behind shock waves on heat transfer and diffusion is studied in the paper. Application of the state-to-state kinetic theory approach allowed estimating the contributions of heat conductivity (Fourier flux), thermal diffusion, mass diffusion and diffusion of vibrationally excited molecules to the total energy flux in the shock heated flows. It is found that compensation effect between heat conduction and diffusion processes results in a considerable reduction of the total heat transfer rate close to the shock front. It is demonstrated that due to differences in the rates of elementary processes in nitrogen and oxygen mixtures, diffusion processes proceed in different ways in these mixtures.

Calculations have been done for free stream Mach numbers $M_0 = 18, 15, 10$ allowing for thermal equilibrium and strong vibrational non-equilibrium before the shock front. The results show that kinetic and dissipative processes proceed more efficiently for higher Mach numbers. With the use of state-to-state flow description, a dramatic impact of strong vibrational excitation of free stream molecules on vibrational-chemical kinetics and heat transfer behind a shock is found for $M_0 = 10$.

The comparison of the results with those found using the one-temperature approach shows a substantial difference between the fluid dynamic variables and fluxes obtained in the frame of the state-to-state and thermal equilibrium kinetic models. It is found that in the vicinity of the shock front the one-temperature approach leads to essential underestimation of the gas temperature and overestimation of atom densities and the absolute value of the total heat flux for both mixtures, the difference decreases with the distance from the shock front.

Strong coupling of kinetic processes, gas dynamic parameters and transport properties in two considered mixtures is demonstrated in the paper. Thus noticeable distinctions in diffusion and energy fluxes for N_2/N and O_2/O mixtures is found in the relaxation zone. In oxygen, fast vibrational relaxation and dissociation lead to the sharp variation of gas-dynamic parameters near the shock front and, as a consequence, to greater values of the total heat flux; mass diffusion becomes one of the dominating processes in O_2/O mixture, especially in the case of initial vibrational non-equilibrium. Finally we conclude that the state-to-state kinetics has a strong effect on the transport properties of non-equilibrium flows. We would recommend that more consideration is given to the transport processes when doing state-to-state flow simulations.

The inverse effect of state-to-state transport processes on the vibrational kinetics has not been studied in the present paper. This challenging task requiring development of efficient computational techniques for calculation of state-to-state transport coefficients in each cell of computational grid represents a subject to our further studies.

Conflict of interest

There are no conflict of interest.

Acknowledgments

This study is supported by the Russian Science Foundation (project 15–19-30016). O. Kunova acknowledges that she is employed by Saint-Petersburg State University in the frame of post-doctoral fellowship 6.50.2522.2013.

References

[1] E. Nagnibeda, E. Kustova, Nonequilibrium Reacting Gas Flows. Kinetic Theory of Transport and Relaxation Processes, Springer, Berlin, 2009.
[2] R. Brun, High Temperature Phenomena in Shock Waves, Shock Wave Science and Technology Reference Library, vol. 7, Springer, Berlin, 2012.
[3] E. Nagnibeda, The structure of the relaxation zone behind shock waves in the reacting gas flows, in: J. Hunt (Ed.), Aerothermodynamics for Space Vehicles, ESA Publications Division, 1995, p. 299.
[4] I. Adamovich, S. Macheret, J. Rich, C. Treanor, AIAA J. 33 (1995) 1064.
[5] F. Lordet, J. Meolans, A. Chauvin, R. Brun, Shock Waves 4 (1995) 299.
[6] E. Josyula, W.F. Bailey, J. Thermophys. Heat Transfer 15 (2001) 157.
[7] O. Kunova, E. Nagnibeda, Chem. Phys. 441 (2014) 66.
[8] O. Kunova, E. Nagnibeda, Chem. Phys. Lett. 625 (2015) 121.
[9] R. Jaffe, D. Schwenke, G. Chaban, Vibration-rotation excitation and dissociation in N_2–N_2 collisions from accurate theoretical calculations, in Proc. 10th AIAA/ASME Joint Thermophysics and Heat Transfer Conference, June 2010 (2010) AIAA Paper 2010–4517.
[10] J. Kim, I. Boyd, Chem. Phys. 415 (2013) 237.
[11] M. Panesi, A. Munafò, T.E. Magin, R.L. Jaffe, Phys. Rev. E 90 (2014) 013009.
[12] A. Ern, V. Giovangigli, Lect. Notes Phys., Ser. monogr., M24, Springer-Verlag, 1994.
[13] A. Chikhaoui, J. Dudon, E. Kustova, E. Nagnibeda, Phys. A 247 (1997) 526.
[14] A. Chikhaoui, J. Dudon, S. Genieys, E. Kustova, E. Nagnibeda, Phys. Fluids 12 (2000) 220.
[15] E. Kustova, E. Nagnibeda, Chem. Phys. 233 (1998) 57.
[16] E. Kustova, E. Nagnibeda, I. Armenise, M. Capitelli, J. Thermophys. Heat Transfer 16 (2002) 238.
[17] I. Armenise, E. Kustova, Chem. Phys. 428 (2014) 90.
[18] E. Josyula, J. Burt, E. Kustova, P. Vedula, Influence of state-to-state transport coefficients on surface heat transfer in hypersonic flows, AIAA Paper 2014–0864 (AIAA SciTech, in: 52nd Aerospace Sciences Meeting, American Institute of Aeronautics and Astronautics, 13–17 January 2014, National Harbor, Maryland), doi:10.2514/6.2014-0864.
[19] M. Capitelli, D. Bruno, A. Laricchiuta, Fundamental Aspects of Plasma Chemical Physics: Transport, Springer Series on Atomic, Optical, and Plasma Physics, vol. 74, Springer Verlag, Berlin, 2013.
[20] G. Colonna, L.D. Pietanza, M. Capitelli, J. Thermophys. Heat Transfer 22 (2008) 399.
[21] I. Nompelis, G.V. Candler, M.S. Holden, AIAA J. 41 (2003) 2162.
[22] R.M. Gehre, V. Wheatley, R.R. Boyce, J. Propul. Power 29 (2013) 648.
[23] G. Chernyi, S. Losev, S. Macheret, B. Potapkin, Physical and Chemical Processes in Gas Dynamics, vol. 1, 2, American Institute of Aeronautics and Astronautics, 2004.
[24] L. Ibraguimova, O. Shatalov, in: R. Brun (Ed.), High Temperature Phenomena in Shock Waves, Springer-Verlag, Berlin Heidelberg, 2012, pp. 99–147.
[25] G. Colonna, M. Capitelli, J. Phys. D: Appl. Phys. 34 (2001) 1812.
[26] G. Colonna, M. Capitelli, J. Thermophys. Heat Transfer 15 (2001) 308.
[27] E. Kustova, Chem. Phys. 270 (2001) 177.
[28] E. Kustova, E. Nagnibeda, T. Alexandrova, A. Chikhaoui, Chem. Phys. 276 (2002) 139.
[29] L. Cutrone, M. Tuttafesta, M. Capitelli, A. Schettino, G. Pascazio, G. Colonna, 3D nozzle flow simulations including state-to-state kinetics calculation, in Proc. of the 29th International Symposium on Rarefied Gas Dynamics 1628, 2014, p. 1154–1161.
[30] E. Kustova, E. Nagnibeda, A. Chauvin, Chem. Phys. 248 (1999) 221.
[31] E. Kustova, G. Oblapenko, Phys. Fluids 27 (2015) 016102.
[32] E. Kustova, G. Kremer, Chem. Phys. 445 (2014) 82.
[33] R. Schwartz, Z. Slawsky, K. Herzfeld, J. Chem. Phys. 20 (1952) 1591.
[34] P. Marrone, C. Treanor, Phys. Fluids 6 (1963) 1215.
[35] L.B. Ibraguimova, A.L. Sergievskaya, V.Y. Levashov, O.P. Shatalov, Y.V. Tunik, I.E. Zabelinskii, Investigation of oxygen dissociation and vibrational relaxation at temperatures 4000–10,800 K, J. Chem. Phys. 139 (2013) 034317.